# The effect of the selective laser melting mode on second phases precipitation in 316L steel during subsequent heat treatment

# The effect of the selective laser melting mode on second phases precipitation in 316L steel during subsequent heat treatment

**D S Popkova*, I M Ruslanov, A Y Zhilyakov, S V Belikov**

Heat Treatment and Physics of Metals Department, Ural Federal University, Ekaterinburg, Russia

*e-mail: d.s.popkova@urfu.ru, a.y.zhilyakov@urfu.ru

**Abstract.** The object of the study was 316L steel obtained by the method of selective laser melting (SLM). The structure of 316L steel was investigated after different SLM modes. The effect of different SLM modes on the second phases precipitation after heat treatment was studied. It is revealed that the fraction of precipitates of the χ-phase correlates with the energy density of the laser beam during SLM.

## 1. Introduction

Selective laser melting (SLM), which belongs to additive technologies or 3D printing methods, is currently an innovative direction in the formation of complex-shaped metal parts. The method of selective laser melting consists in layer-by-layer synthesis of an object due to automatically controlled scanning of microlayers of a powder material with high-energy laser radiation [1].

Using the SLM method, it is possible to obtain products of almost any configuration, however, with size restrictions dictated by the technical features of the SLM installation. The properties of a part made by the SLM method, as well as its structure, depend on many technological parameters. Currently, there are up to 120 different factors affecting the quality and characteristics of objects obtained by the SLM method [2, 3].

The SLM technology has a number of obvious advantages: it makes it possible to create products of the most complex shapes, does not require complex preliminary operations such as design and manufacture of expensive tooling.

The unique conditions for powder crystallization during SLM, namely, ultrafast cooling rates from the state of a liquid metal, as well as multiple thermal cycling, lead to the formation of nonequilibrium structures [4-7].

316L steel has a wide range of applications due to its high corrosion resistance, durability, high strength and ductility. Products made of 316L steel are successfully used in the chemical, petrochemical, mining industries, as well as in the food, jewelry, medical and some other industries. Thanks to the dynamically developing additive technologies of the 21st century, it is possible to expand the scope of this steel due to its unique set of properties.

Thus, the aim of this work is to study and analyze the effect of selective melting modes on the kinetics of the precipitation of second phases in 316L steel.

## 2. Material and research methods

316L corrosion-resistant alloy was used as a material for research. Table 1 shows the chemical composition of the investigated steel.

**Table 1.**The chemical composition of 316L steel

| Content by elements, wt % | | | | | | | | | |
|---|---|---|---|---|---|---|---|---|---|
| C | Mn | P | S | Si | Ti | Ni | Mo | Cr | Fe |
| up to 0.03 | up to 2.0 | up to 0.045 | up to 0.03 | up to 1.0 | up to 0.5 | 10.0…14.0 | 2.0…3.0 | 16.0…18.0 | Bal. |

To achieve the set tasks, metal samples of 316L steel obtained under various operating conditions of the operating conditions installation were investigated.

Table 2 shows the operating conditions of SLM samples of 316L steel.

**Table 2.** SLM modes and samples properties

| № Mode | Laser power, W | Scanning speed, mm / s | Hatch distance, μm | Step in the contour, μm | Layer thickness, μm | Energy density J / mm$^3$ |
|---|---|---|---|---|---|---|
| **1** | 340 | 850 | 80 | 70 | 50 | 115 |
| **2** | 374 | 850 | 80 | 70 | 50 | 110 |
| **3** | 294 | 700 | 80 | 70 | 50 | 105 |
| **4** | 280 | 700 | 50 | 70 | 50 | 160 |

Metal samples of 316 L steel were pre-annealed in air in a SNOL muffle furnace at a temperature of 700 °C with a holding time of 100 hours, followed by a water quenching. Metallographic analysis was performed using an Epiphot 200 optical microscope at magnifications of 100 ... 1000 times.

Metallographic analysis was carried out using a ThermoFisherScios 2 scanning electron microscope. The chemical composition of different zones of samples and inclusions was determined by X-ray spectral microanalysis (MRSA), which was performed on a Jeol JSM-6490LV scanning electron microscope equipped with Oxford Inca Energy 350 energy dispersive microanalyzers at an accelerating voltage of 20 kV.

## 3. Results and discussion

Fig.1 shows the samples structure after SLM across the growing direction.

The melt baths in this section have the shape of an ellipse, and they are integrated into tracks in two mutually perpendicular directions. The track width is on average 80 μm, which corresponds to the “Hatch distance” (from the parameters of the SLM mode).

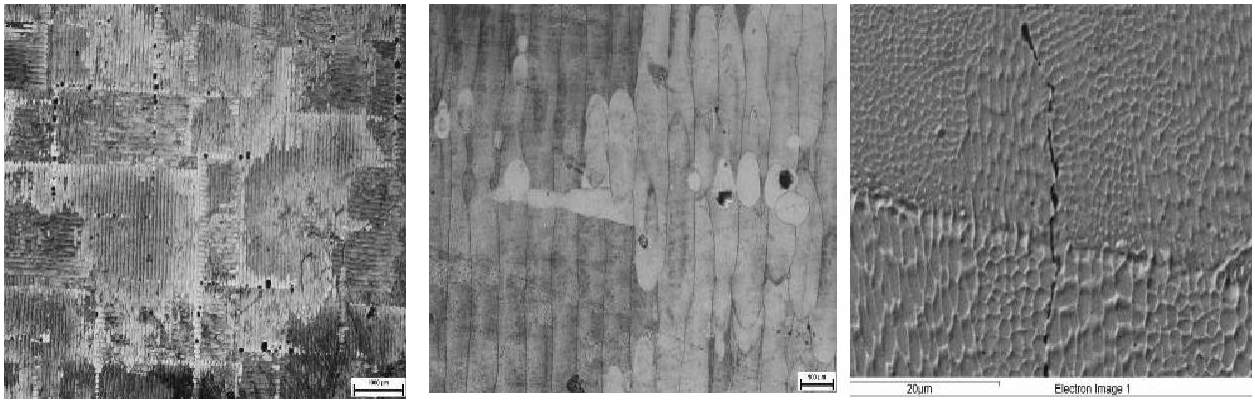


a b c

**Figure 1.** Samples microstructure after SLM across the growing direction.
(a,b -optical micrographs, c- SEM)

Along the growth direction, the melt baths have the form of arcuate segments (Figure 2), the width of which is about 80 μm and coincides in size with the hatch distance. The depth of the baths corresponds to the layer thickness and is about 50 μm.

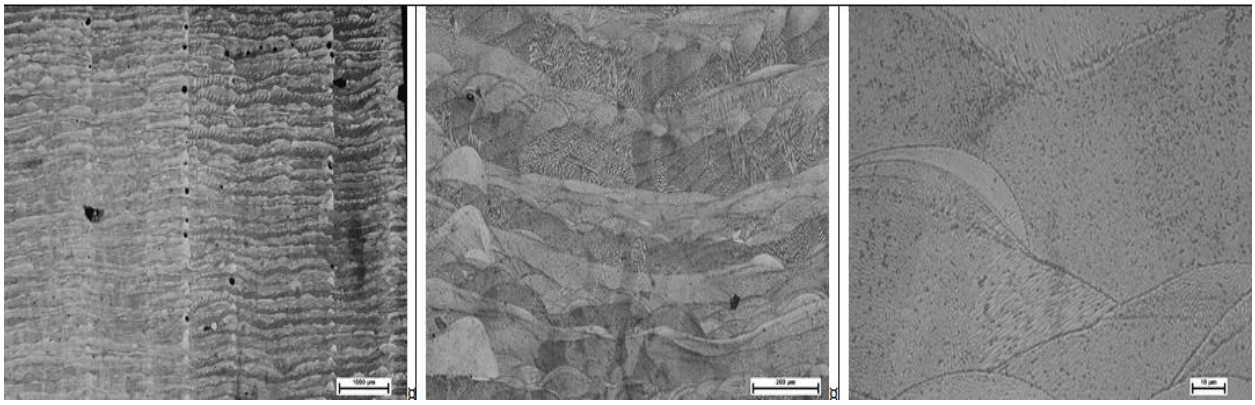

a b c

**Figure 2.** Optical micrographs showing the samples microstructure after
SLM along the growing direction.

It should be noted that during holding at 700 ° C for one hundred hours, precipitates of the second phase appeared in the sample. They are located both along the boundaries and in the body of the austenite grains. They have an elongated rounded shape - along the borders, acicular - in the body of the grain.

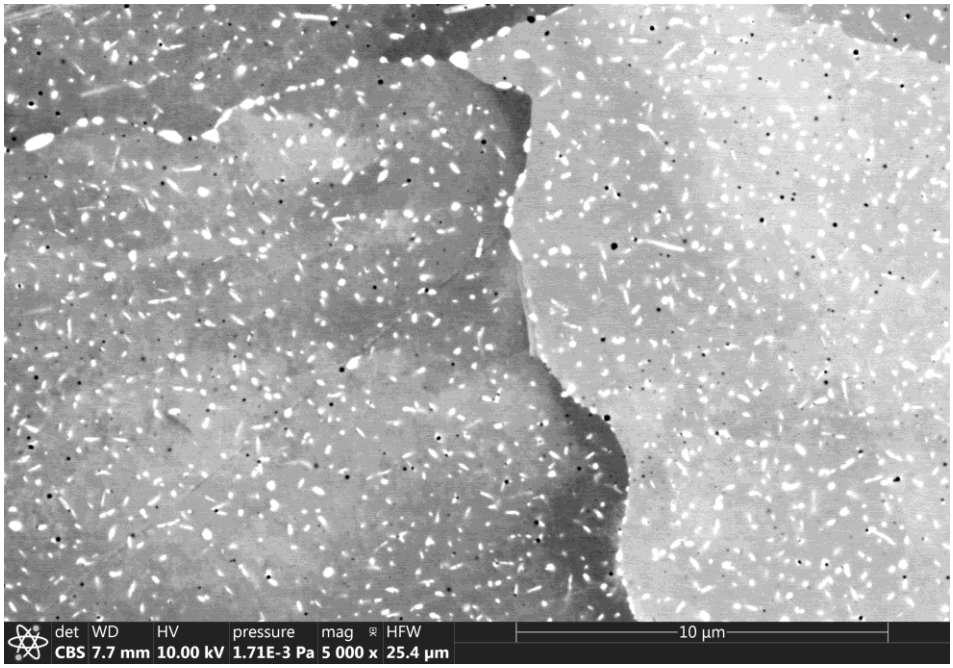


a

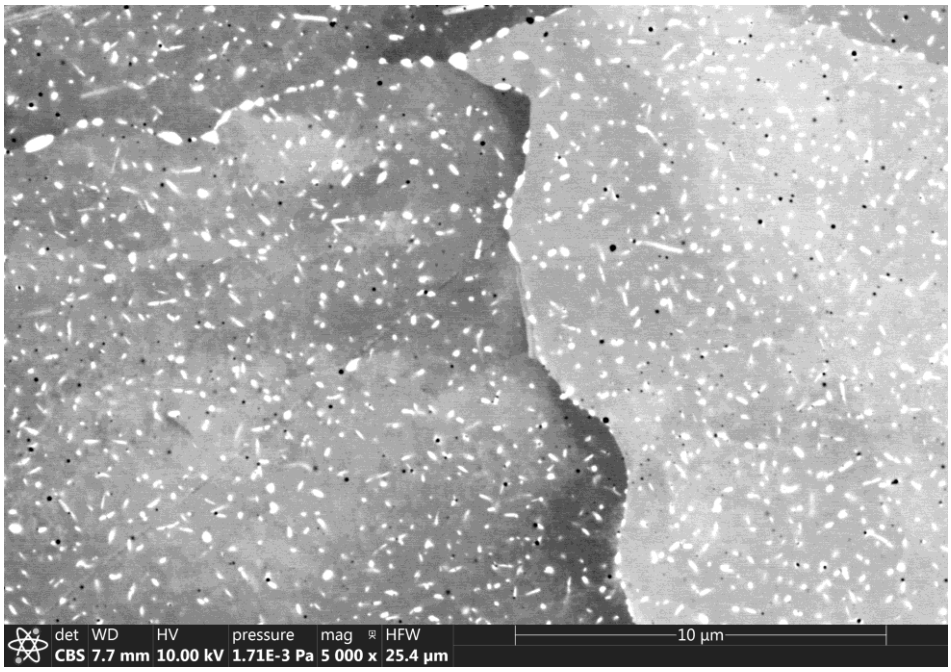


b

**Figure 3.** SEM images showing the second phase precipitation

The contrast on a black and white background for the χ-phase and carbides of the $Me_{23}C_6$ type was obtained using the binarization function - a kind of digital raster images, when each pixel can represent only one of two image colors.

The evaluation of pixels occupied by the χ - phase and carbides of the $Me_{23}C_6$ type from the total space was performed using a graphical editor.The total space occupied by the χ - phase and carbides of the $Me_{23}C_6$ type of the total pixel volume was found using the proportion.

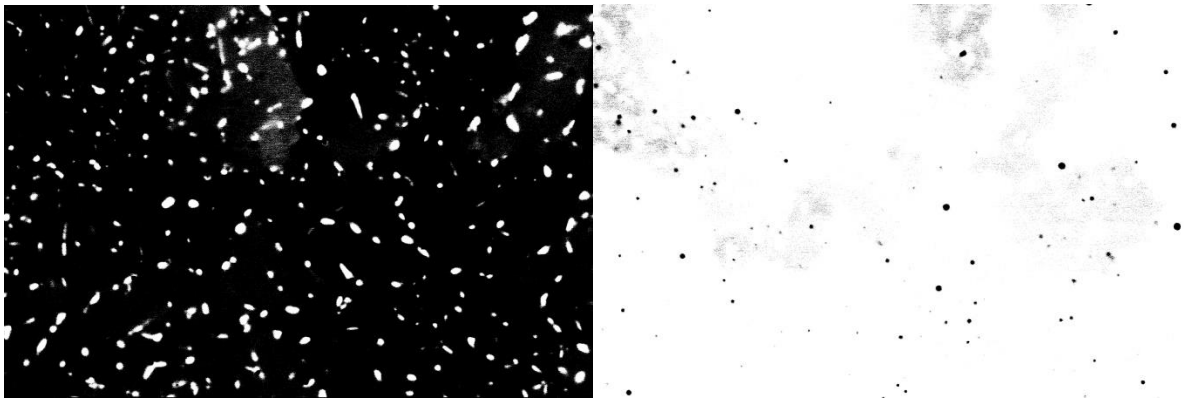

a b

**Figure 4.** SEM images showing the χ – phase precipitation(a) and carbides of the $Me_{23}C_6$ type (b) after graphical editor (SLM mode 1)

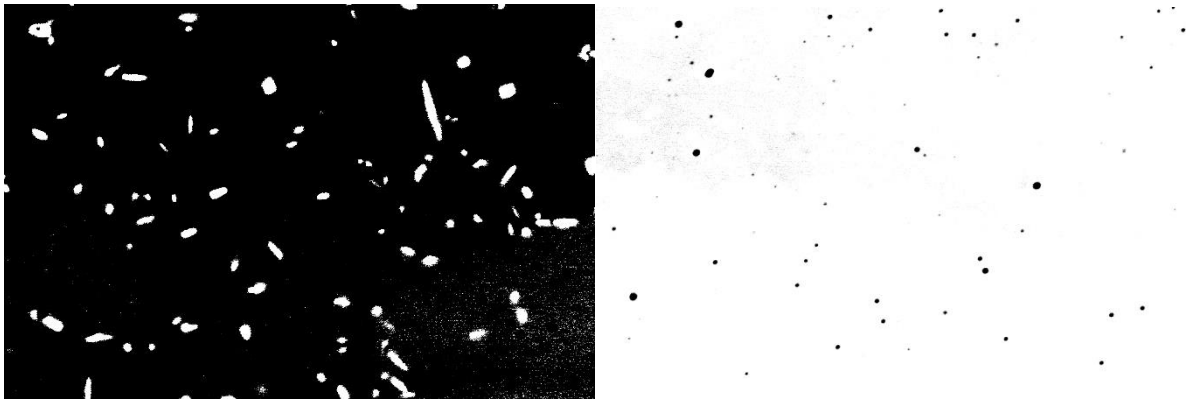

a b

**Figure 5.** SEM images showing the χ – phase precipitation(a) and carbides of the $Me_{23}C_6$ type (b) after graphical editor (SLM mode 2)

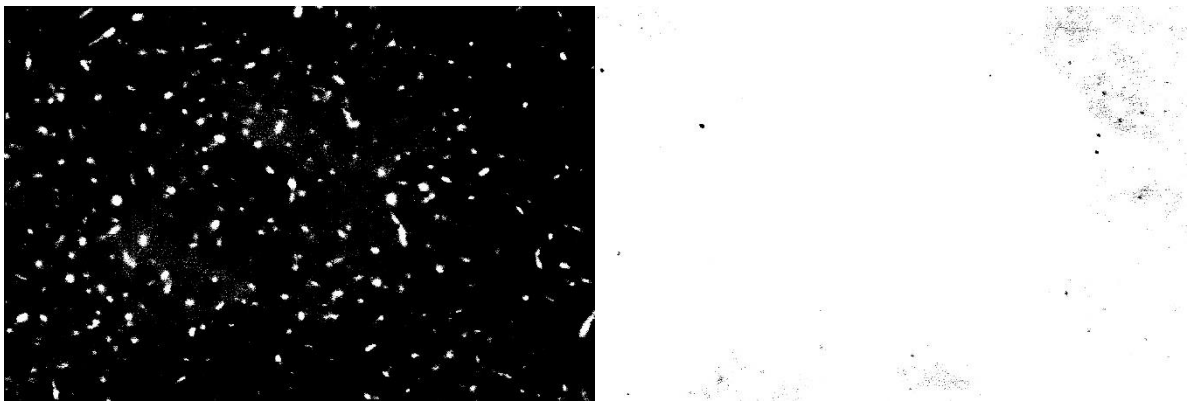

a b

**Figure 6.** SEM images showing the χ – phase precipitation(a) and carbides of the $Me_{23}C_6$ type (b) after graphical editor (SLM mode 3)

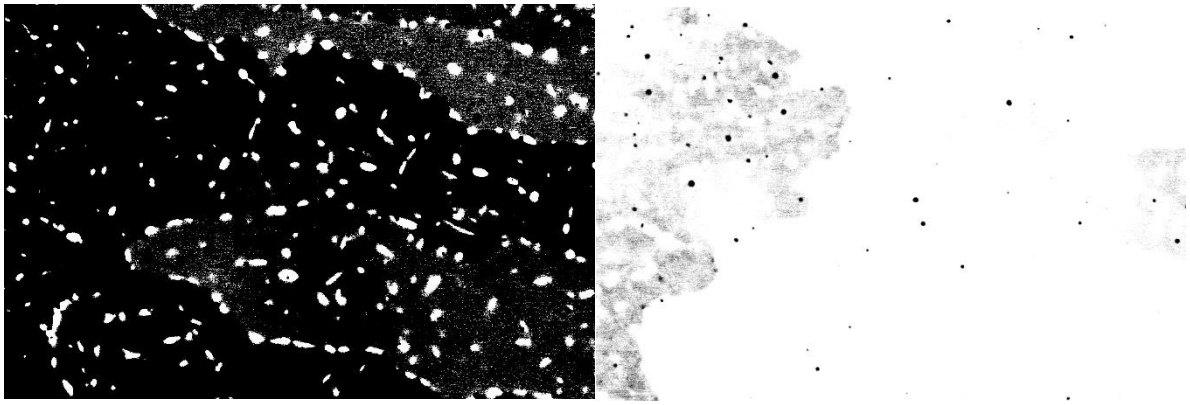

a b

**Figure 7.** SEM images showing the χ – phase precipitation (a) and carbides of the $Me_{23}C_6$ type (b) after graphical editor (SLM mode 4)

**Table 3.** The effect of different SLM modes on the precipitation of the second phases

| SLM mode | χ -phase,% | $Me_{23}C_6$,% |
|---|---|---|
| 1 | 5,22 | 0,314 |
| 2 | 3,13 | 1,05 |
| 3 | 2,71 | 0,047 |
| 4 | 6,65 | 0,33 |

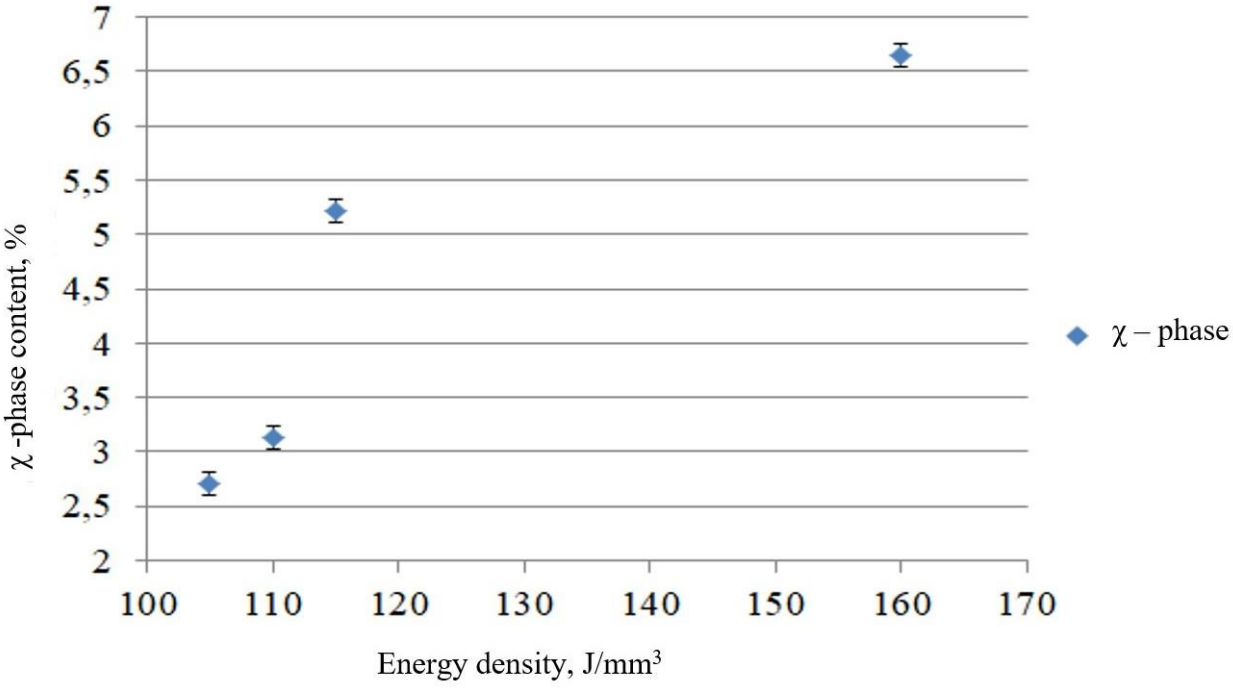


**Figure 8.** Dependence of the χ -phase volume fraction on energy density.

## 4. Conclusions

- It was shown that the use of the SLM method led to the formation of a cellular structure in 316L steel.
- It was revealed that an increase in the energy density did not lead to an increase in the precipitation of carbides of the $Me_{23}C_6$ type.
- It was found that with an increase in the energy density, the volume fractionof χ-phase precipitation increased. The volume fraction of χ-phase precipitation reached its maximum values under the SLM mode providing an energy density of 160 J / $mm^3$.

## Acknowledgments

The research was carried out with the support of the project "Creation and functioning of a network of international scientific and methodological centers for the dissemination of the best international practices for the training, retraining and internship of advanced digital economy personnel in the fields of mathematics, computer science, technology" (Agreement No. 075-15-2019-1907 dated 09.12.2019).

## References

[1] Shishkovsky I 2009 Laser synthesis of functional-gradient mesostructures and bulk products (Moscow: FIZMATLIT) 424 [in Russian]
[2] Santos E 2006 International Journal of Machine Tools & Manufacture **46** 1459–1468
[3] Zakiev S 2006 *Appl. Phys. A* **84** 123–129
[4] Yasa E and Kruth J-P 2011 *Procedia Engineering* **19** 389–95
[5] Sun Y 2014 *JMEPEG* **23** 518–526
[6] Li R 2010 *Applied Surface Science* **256 (13)** 4350–4356
[7] Kempena K 2011 *Physics Procedia* **12** 255–263
[8] Islam M 2013 *Physics Procedia* **41** 828–835
[9] Wang D 2012 *Int. J. Adv. Manuf. Technol.* **58** 1189–1199
[10] Nakamoto T 2009 Journal of Materials Processing Technology **209** 5653–5660
[11] Li R 2010 *JMEPEG* **19** 666–671
[12] Li R 2012 *Int. J. Adv. Manuf. Technol.* **59** 1025–1035
[13] Ciurana J 2013 *Int. J. Adv. Manuf. Technol.* **68** 1103–1110
[14] Pupo Y 2013 *Procedia Engineering* **63** 370–378
[15] Delgado J 2012 *Int. J. Adv. Manuf. Technol.* **60** 601–610
[16] Baicheng Z 2012 *Materials and Design* **34** 753–758
[17] Olakanmi E 2013 Journal of Materials Processing Technology **213** 1387–1405